Scientific Research Publishing

Atmospheric and Climate Sciences, 2025, 15(4), 761-787
https://www.scirp.org/journal/acs
ISSN Online: 2160-0422
ISSN Print: 2160-0414

Spatiotemporal Analysis of Aerosol Optical Properties and Their Associations Using Satellite and Ground-Based Observations

Dennis W. Wanjala*, John W. Makokha, Geoffrey W. Khamala

Department of Science, Technology and Engineering, Kibabii University, Bungoma, Kenya
Email: *makokhajw@kibu.ac.ke

How to cite this paper: Wanjala, D.W., Makokha, J.W. and Khamala, G.W. (2025) Spatiotemporal Analysis of Aerosol Optical Properties and Their Associations Using Satellite and Ground-Based Observations. *Atmospheric and Climate Sciences*, **15**, 761-787.
https://doi.org/10.4236/acs.2025.154039

Received: July 7, 2025
Accepted: September 26, 2025
Published: September 29, 2025

Abstract

Aerosols play a critical role in Earth's climate system. They influence cloud formation, atmospheric dynamics and Earth's energy balance. This study presents a comprehensive spatiotemporal analysis of aerosol optical depth (AOD), Angstrom Exponent (AE), Single scattering Albedo (SSA) and their associations with primary climate variables such as Surface Air Temperature (SAT) and Rainfall Rates (RR). The present study derived its data from both satellites based remote sensing data and ground based observation, *i.e.*, Moderate Resolution Imaging Spectrometer (MODIS), Modern Era Retrospective Analysis for Research and Application 2 (MERRA-2) and Tropical Rainfall Mission (TRMM) between the years 2000 to 2022. These data platforms are run and maintained by National Aeronautics and Space Administration (NASA). The researcher examined monthly and annual trends. Hidden Markov models were employed to determine the patterns and potential cause of variabilities and the link between aerosol optical properties and climate variables. The researcher determined trends in AOP and evaluated the trends in climate variables using HMM. Satellite-based dataset provided enhanced spatial resolution, accurate and observation. The findings gave more insight into aerosol dynamics and accurate climate modelling; the researcher addressed critical gaps in understanding the interactions between aerosols and climate variables in Kenya, a region highly vulnerable to the impacts of climate change and air quality degradation, hence better environment planning policy. Identified hidden patterns and transitions that were often overlooked by traditional methods. The methodological innovation is not only relevant for Kenya but also adaptable to other regions facing similar environmental challenges, thereby contributing to the broader field of atmospheric sciences.

Keywords

MODIS, MERRA-2, TRMM, HMM, Kenya

1. Introduction

Aerosols are tiny particles or liquid droplets suspended in the atmosphere, they are key players in the Earth's climate system [1] [2]. Aerosols play a critical role in shaping the climate system of a particular region. They influence the environment through their interactions with solar radiation, cloud formation, and atmospheric dynamics, exerting both cooling and warming effects on the planet's surface [3]-[7]. Aerosol impact is especially pronounced in regions such as Kenya, where diverse aerosol sources, ranging from natural dust emissions to biomass burning and urban pollution create a complex interplay between human activities and atmospheric processes [8]. This complexity underscores the need for detailed investigations into aerosol optical properties (AOPs) and their associated climate variables to understand the implications for regional climate variability and resilience.

The aerosol-climate nexus is particularly relevant to Kenya due to its unique geographical and climatic characteristics. Positioned within the Greater Horn of Africa, Kenya experiences highly variable weather patterns governed by monsoonal flows, the Intertropical Convergence Zone (ITCZ), and orographic influences from highland areas such as the Mau Forest Complex and the Rift Valley [9]. These factors, combined with seasonal events such as biomass burning and dust transport, contribute to episodic aerosol loading that affects precipitation, surface temperatures, and overall atmospheric dynamics. For instance, high aerosol optical depth (AOD) events have been linked to reduced rainfall, prolonged droughts, and intensified flooding, all of which have far-reaching consequences for agricultural productivity, water resources, and human health [10].

Aerosol optical properties such as AOD, single scattering albedo (SSA), and Angstrom Exponent (AE) provide valuable insights into the nature, concentration, and radiative effects of aerosols. AOD quantifies the extent to which aerosols block sunlight, while SSA measures their scattering versus absorbing capabilities, while the AE helps differentiate particle size distributions [7] [11]. However, detecting anomalies in these properties defined as deviations from expected patterns, is challenging due to their inherent variability and the limitations of observational datasets, particularly in regions with sparse monitoring infrastructure like Kenya. The increasing availability of remote sensing data from sources such as satellite, modelled and ground platforms provides an unprecedented opportunity to overcome these challenges and improve our understanding of aerosol behaviors and their climatic effects [3].

Detecting anomalies in AOPs was critical for identifying extreme aerosol events, such as dust storms, wildfire smoke plumes, and urban pollution episodes,

which have significant implications for regional climate systems. Traditional approaches often struggle to capture the nonlinear, dynamic, and multivariate nature of atmospheric datasets. Hidden Markov Models (HMMs), statistical tools designed to uncover hidden states in time-series data, have emerged as a powerful framework for addressing such complexities [12] [13]. HMMs excel in modelling temporal dependencies and transitions between normal and anomalous states, making them particularly suited for analyzing aerosol time-series data and their interactions with climate variables [14] [15].

The study employed HMMs to investigate trend analysis in Aerosol Optical Properties such as AOD, SSA, AE and associated climate variables as Rainfall Rates (RR), and Surface air Temperature (SAT) over Kenya and further detection of anomalies in the forementioned properties and climate variables over the same domain [16]. By integrating satellite observations, modelled and ground-based measurements, the research elucidated the temporal and spatial variability of aerosols and their climatic impacts. Kenya's climate challenges marked by recurrent droughts, flooding, and shifting rainfall patterns necessitated a deeper understanding of the aerosol-climate relationship to inform mitigation and adaptation strategies [8]. Moreover, addressed aerosol-related challenges aligns with Kenya's broader commitments to sustainable development goals, particularly in areas such as air quality, climate resilience and food security.

2. Study Area, Data and Methods

2.1. Study Area

Kenya, bounded by Latitudes 5˚S - 5˚N and Longitudes 34˚E - 42˚E, a country in East Africa bordered by Ethiopia to the North, Tanzania to the South, South Sudan to the Northwest, Uganda to the West and Somalia to the East. Climatologically, the area is predominantly tropical with four seasons categorized according to rainfall patterns [17]. For instance, March-April-May (MAM) and October-November-December (OND) are local wet seasons characterized with low AOD due to enhanced wet scavenging and reduced anthropogenic activities [2]. On contrary, the local dry seasons January-February (JF) and June-July-August-September (JJAS) are characterized by high AOD attributed to changes in meteorological conditions, emission sources and reduced wet deposition [2] [18] [19] (**Figure 1**).

2.2. Data

This section presents the suitable methods used to analysis data retrieved from data platforms TRMM, MODIS and MERRA-2 in order to get meaningful information from the data obtained.

2.2.1. Moderate Resolution Imaging Spectroradiometer (MODIS)

MODIS is a satellite sensor brought into the Earth's atmosphere by the National Aeronautics and Space Administration (NASA) in partnership with Goddard

Space Flight Centre (GSFC). It is divided into MODIS Aqua which orbits at 13:30 p.m. local time and MODIS Terra orbiting at 10:30 a.m. local time. Using a temporal resolution of 1 - 2 days and a swath of 2330 km, MODIS obtains its data in 36 bands. Out of the 36 bands, 5 bands are at 500 m, 2 bands at 250 m and 29 bands at 1 km [20]-[22] with two algorithms: Deep Blue (DB) and Dark Target (DT). Recently, MODIS AOD product over land is operational on Collection 6.1 [23]. They record large-scale geodynamic processes, *i.e.*, changes in cloud cover, radiation budget, and also provide information about the deeper atmosphere and Oceans.

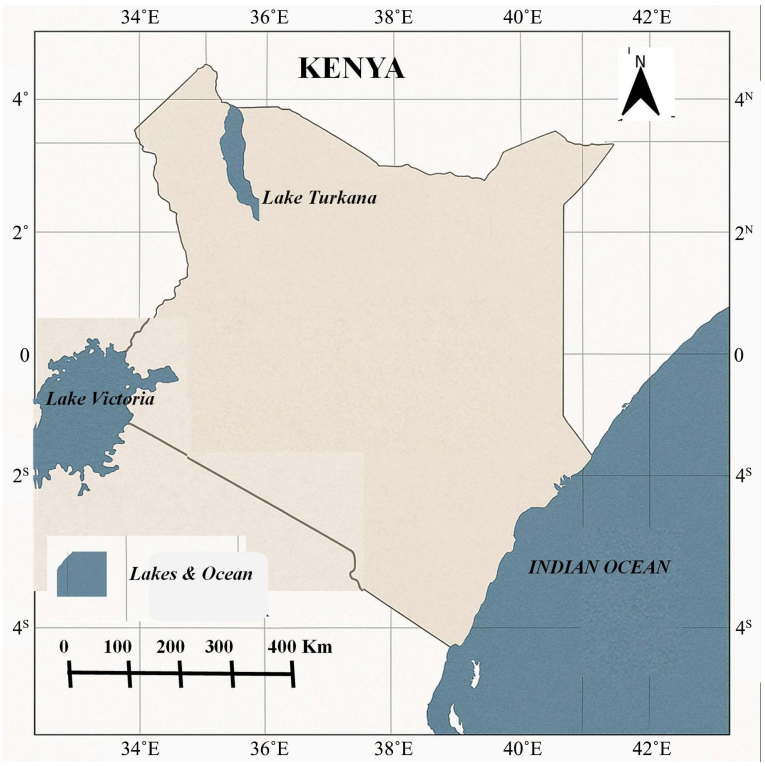

Figure 1. Map of Kenya showing study area (Drawn by authors).

2.2.2. Modern Era Retrospective Analysis for Research and Application Version 2 (MERRA-2)

(MERRA-2) is the latest atmospheric reanalysis of the modern satellite era produced by NASA Global Modelling and Assimilation Office [24]. MERRA-2 production began in June 2014 in four processing streams, and converged to a single near-real time stream in mid-2015. Its products can easily be accessed online through the NASA Goddard Earth Sciences Data Information Services Centre (GESDISC). Data website MERRA-2 assimilates observation types not available to its predecessor, MERRA, which includes updates to the Goddard Earth Observing System (GEOS) model and analysis scheme so as to provide a viable ongoing climate analysis beyond MERRAs terminus [25]. MERRA 2, was designed to address limitations of MERRA, and additionally, it also intended to be a development milestone for a future integrated Earth system analysis (IESA) which is cur-

rently under development at GMAO. Among the advances in MERRA-2 relevant to IESA are the assimilation of aerosol observations, several improvements to the representation of the stratosphere including ozone, and improved representations of cryosphere processes. Other improvements in the quality of MERRA-2 compared with MERRA include the reduction of some spurious trends and jumps related to changes in the observing system, and reduced biases and imbalances in aspects of the water cycle [26].

2.2.3. Tropical Rainfall Measure Mission (TRMM)

Tropical Rainfall Measure Mission (TRMM) is a joint project that was established and launched 1997 between NASA and the Japanese space agency, JAXA. TRIMM provides the research and operational communities' unique precipitation information from space. Use of both active and passive microwave instruments and processing, low inclination orbit (35˚) makes TRMM the world's foremost satellite for the study of precipitation and associated storms and climate processes in the tropics. TRMM is designed to measure rain rates from space using a combination of high-resolution radar, passive microwave radiometer and visible-infrared radiometer measurements from a spacecraft in a rapid precession. These measurements, averaged over a 500 km grid for a month, are expected to provide monthly mean rainfall to an accuracy of 10 - 15 percent [27]. The TRMM provides visible, infrared, and microwave observations of tropical and subtropical rain systems, as well as lightning and cloud and radiation measurements. The satellite observations are complemented by ground radar and rain gauge measurements to validate satellite rain estimation algorithms [28]. The TRMM rain sensor package includes the first space-borne Precipitation Radar (TPR), a TRMM Microwave Imager (TMI) and a Visible and Infrared Scanner (VIRS). Rainfall estimates provided by the TRMM have found applications in climate analysis, data assimilation, water resource management, and decision support to agriculture and health issues [29]. The precipitation radar on-board the TRMM satellite is the first space borne radar to measure precipitation from space.

2.3. Methodology

2.3.1. Descriptive Statistical Analysis

Provided a foundational understanding of the distribution, central tendency and variability of aerosol optical properties and associated climate Variables SAT and RR. In this study, descriptive statistical analysis was employed to examine both temporal and spatial patterns over Kenya 2000-2022. Mean ($\overline{x}$) was used to identify central value of AOD, AE, SSA, SAT and RR over monthly and yearly intervals.

$$\overline{x} = \frac{1}{n\sum_{i=1}^{n} xi} \tag{1.1}$$

$\overline{x}$ = mean of AOD, SSA, AE, SAT and RR. xi = individual observation, n = number of observations.

Standard deviation assessed degree of variability of data around the mean highlighting regions of high climate fluctuation.

$$\sigma = \sqrt{\frac{1}{n}\sum_{i=1}^{n}\left(x_i - \overline{x}\right)^2} \tag{1.2}$$

Coefficient of variation (CV) was used to compare variability across different variables and regions in Kenya. Expressed as a ratio of standard deviation to mean.

$$\mathrm{CV} = \frac{\sigma}{\overline{x}} \times 100\% \tag{1.3}$$

Minimum and maximum value was used to identify the range and extremes of each variable and capture instances of drought, heavy rainfall and high aerosol loading in the region [30].

Temporal analysis: Time Average Maps plots and description summaries were used to analyze variabilities and long-term shifts in AOD, SSA, SSA, SAT and RR. Seasonal mean average mean used to highlight annual fluctuations.

Spatial Analysis: Spatial averaging and zonal statistics were applied across different Climatic zones in Kenya to capture regional variability. Time Average Maps were plotted means and standard deviation were generated to visualize spatial patterns and identify hotspots for extreme aerosol loading. Using the Maps regions with consistent aerosol loading and extreme climate variability were identified.

2.3.2. Linear Regression Analysis

It was used to identify and quantify temporal trends. Linear regression was applied to assess long-term trends in AOD, SSA, and AE, and their association with SAT and RR over Kenya (2000-2022), determining the likelihood of each variable to increase, decrease, or remain stable at each spatial grid point.

$$Y_t = \beta_0 + \beta_1 t + \epsilon_t \tag{1.4}$$

Y_t value of variable at time t, t time in month/year; β_0 value at the start of period. β_1 trend per time.

$\beta_1 > 0$ increasing trend $\beta_1 < 0$ decreasing trend ϵ_t error term

$\beta_1 \approx 0$ No significant trend

Trends significance testing. To assess the statistical significance of the trend, a t-test was used on the slope coefficient. The null hypothesis.

$$Ho : \beta_1 = 0 \text{ Test at } 95\%$$

Confidence level

$$\beta < 0.05$$

3. Results and Discussion

3.1. Trend in Aerosol Optical Depth (AOD)

The trends in AOD over the study domain are depicted in **Figure 2**. Generally, an increase in AOD trend shown by Positive values while negative values indicate a decreasing trend in AOD. To start with, January (**Figure 2(a)**) between 1 - 2˚N

and 36 - 39˚E, the region experienced a strong increasing AOD trends which could be attributed to the reduced wet deposition and increased dust emission in the region [2] [7]. Eastern Kenya had areas of weak decreasing trends in AOD which could be attributed to minimum dust loading and light down pouring [31]. January to March. January AOD trend, Western and Nyanza region experienced an increase in AOD > 0.001 year^{-1}, which could be attributed to increased dust loading, the ground in very dry hence too much dust emission [31].

Towards the Rift valley, the AOD decreased to <0.001 year^{-1}, Eastern region AOD decreased to <−0.001 year^{-1} recording to almost −0.002 year^{-1} trend January is within the dry months but with negative anomalies this can be attributed to decrease in biomass burning, variation in soil moisture and changes in rainfall pattern within the region [2]. Coastal and North eastern region recorded an increase in AOD with values > 0.002 year^{-1} with some areas recording 0.003 year^{-1} January the coastal region is very dry, with increased anthropogenic activities within the coastal region, including biomass burning, emission of dust, emission from industries and motors emission could have contributed to this great increase in AOD [2] [31].

February (**Figure 2(b)**) Nyanza region recorded an increasing AOD trend > 0.001 year^{-1}, with some area especially around the Lake with higher AOD values of 0. 002 year^{-1} this can be attributed to high dust emission, higher evaporation rate due to high SAT within the region, dust emission due to very little moisture content in the soil [2] [31]. Rift valley and region around the equator, the AOD decreases as one moves towards the Eastern region, recording values less than −0.001 year^{-1}, the decrease could have been contributed by the fact that one is moving from lower altitude to higher altitude, with relatively higher vegetation cover hence less dust emission and biomass burning [19]. North eastern region, some area showed an increase in AOD especially when one moves toward the areas bordering Somalia country attributed to influence of dust from arid and semi-arid regions transported by strong winds especially from Arabian Peninsula [32].

March (**Figure 2(c)**) 2000-2022, The country experienced a greater decrease in AOD of <−0.001 year^{-1} in majority of areas. Northern part of Kenya experienced a greater decrease in AOD with majority of region North Rift, North Eastern with values < −0.002 year^{-1}, this is attributed to meteorological factors that have a great influence on the variability and seasonality of the AOD; wet months there is increased rainfall washout, minimum dust loading factored to moisture content in the soil [31]. Region around the Equator recorded a slight increase in AOD of >0.002 year^{-1} which was a positive anomaly attributed to low rainfall patterns within the region [2].

April (**Figure 2(d)**) 2000-2021 Majority of the region experienced a negative anomaly in AOD with only a smaller area with Eastern Region showing an increase in AOD greater than 0.001 year^{-1}. April is within wet months, increased rainfall washout, during April, there is maximum moisture content in the soil, hence dust emission is very low, biomass burning is very minimum thus decreasing trend in AOD [31].

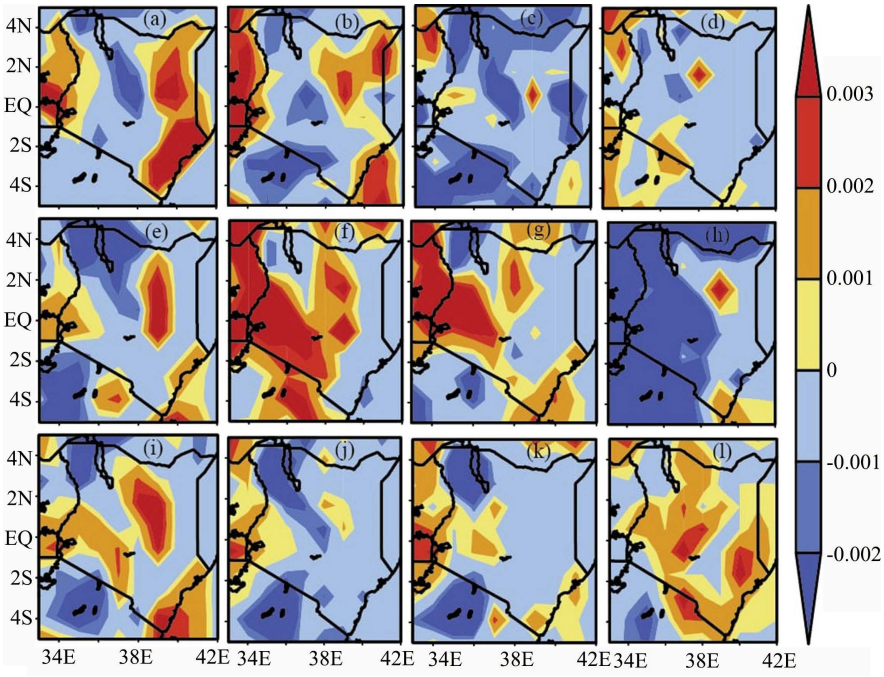

Figure 2. Present time average map for combined dark target and deep blue AOD at 0.55 micron for land and ocean monthly deg. [MODIS-Terra] over 2000-2022.

May (**Figure 2(e)**) Nyanza and Western Kenya recorded an increase AOD trend, North Rift, especially region around Lake Turkana and as one approach towards Sudan. Nyanza region especially region around Mbita, its dominance of absorbing fine mode aerosols could have led to an increase [7]. Western region this could have been attributed by increase in industrial emission with the presence of paper industry and several sugar industries, factories emission and vehicle emission [33]. AOD decreased with a larger value with some areas recording AOD less than −0.002 year^{-1}, a large negative anomaly observed wet month hence increase in rainfall downpour resulting to decrease in dust emission [2]. Eastern region recorded an increasing AOD trend of greater than +0.002 year^{-1}, with some area recording values above +0.003 year^{-1} attributed to influence of dust from Arid and semi-arid region. Eastern is semi-arid hence more dust emission to the atmosphere [32]. North-eastern experienced a negative anomaly towards Somalia boarder. Coastal region showed an increasing AOD trend. Changes in wind patterns transporting aerosol from distance sources to the coastal region [33].

June (**Figure 2(f)**) 2000-2022, Majority of the regions experienced an increase in AOD with values greater than +0.002 year^{-1}. Western and Nyanza Region recorded the largest values, almost in all areas within the region, this could have been attributed by decline in rainfall hence increasing moisture content in the atmosphere, increase in anthropogenic activities coupled with prevailing climatic conditions, thus affecting the values of AOD in the atmosphere [2] [7]. North Rift experienced a decreasing trend, and major part of Northeastern and coastal region. For North Rift this could be attributed to increase in altitude hence less AOD [19].

July (**Figure 2(g)**) 2000-2022, Western, part of Rift valley, Nyanza, Central region recorded an increase in AOD in some areas within the region. Region around the equator recorded an increase in AOD of greater than 0.002 attributed to change in rainfall pattern, since July is within dry months with little downpour [2]. North eastern, coastal Region and areas around Lake Turkana recorded a decrease in AOD of −0.001 year^{-1} change in wind pattern transporting aerosol from the region to distance area towards Sudan [33].

August (**Figure 2(h)**) 2000-2022, The country experienced a decrease in AOD in majority of the region with values less than −0.002 year^{-1} this could be attributed to decrease in Biomass burning and agricultural practices such as land clearing which involves burning, also August experiences rainfall hence reducing water vapor in the atmosphere [32]. A small region within North Eastern showed increasing in AOD of >0.002 year^{-1}, small region in coastal area recorded a positive anomaly attributed to changes in wind patterns transporting aerosols from distance regions to this area [32] [33].

September (**Figure 2(i)**) 2000-2022, North rift, region towards Sudan, negative AOD of −0.002 year^{-1} effect of Northern winds is less pronounced in the region leading to drop in AOD trends, there is also a factor of change in wind patterns hence carrying fine particles to regions away [33]. Central Kenya, and some parts of Rift valley recorded an increasing in AOD of 0.001 year^{-1}, Part of Eastern region, majority of the area recorded an increase in AOD of >0.002 year^{-1} attributed to increasing anthropogenic activities, coupled with the prevailing climate conditions [2]. Coastal region observed an increase in AOD values, >0.001 year^{-1}. North Eastern, Part of Rift Valley, Eastern, Nyanza, recorded a decreasing trend, this can be attributed to migration of *aerosols* from regional sources, dominance of natural sources such as geothermal activities and low stringent levels [31].

October (**Figure 2(j)**) Central Kenya, Nairobi, parts of Rift Valley, North Eastern, Parts of Eastern, recorded a decreasing trend in AOD of >−0.001 year^{-1}, October is within the wet months, the ground is very wet hence less fine particle emission, at the same time anthropogenic activities would have reduced greatly [33]. North rift recorded the highest negative anomaly of less than −0.002 year^{-1} attributed to changes in wind patterns carrying fine particles away from the region. Very small region in Nyanza, Western and Eastern, recorded an increase in AOD of >0.001 year^{-1} decrease in rainfall pour, variation in wind direction carrying water vapour molecules towards the land region around the Lake [19].

November (**Figure 2(k)**) 2000-2022, majority of the region recorded a decreasing trend in AOD with North rift recording the highest negative value −0.002 year^{-1} attributed to variation in North winds towards Sudan hence carrying aerosols away [33]. Region around the Equator, Nairobi and Coastal region showed a slight increase in AOD, a positive anomaly >0.001 year^{-1}, there is a decline in rainfall, dust emission has increased, Nairobi being highly populated, more biomass burning, industrial area emitting a lot of fine aerosols, motor emission hence an increase in AOD [2] [7].

December (Figure 2(l)) 2000-2022 majority of the region recorded an increase in AOD of >0.001 year^{-1}, central, Nairobi and some costal part recorded values > 0.002 year^{-1}. Some Parts of Nyanza, North rift, Eastern and North eastern, recorded a negative anomaly, decreasing trend in AOD. AOD increase in December can be attributed to decrease in rainfall, the ground is very dry hence loose dust particles, variation in wind direction bringing in more particles from different regions. Increase in biomass burning, land clearing process, more industrial BC emission [32].

3.2. Trends in Angstrom Exponent (AE)

The color scale on the right indicates the magnitude of the trends in AE. Blue shows decreasing trends, Yellow Near zero trend Stable AE, Red shows increasing trends in AE North Rift region around Lake Turkana showed a positive trend up to 0.004 in all plots. More pronounced in January (Figure 3(a)), February (Figure 3(b)), March (Figure 3(c)) and between May (Figure 3(e)) to December (Figure 4(l)) North eastern Kenya showed an increasing trend in AE. Increase in angstrom exponent > 0.002 year^{-1} marked with red was evidenced in Northern parts of Kenya. Showing a positive anomaly in AE. This can be attributed to biomass burning peaking during dry seasons January (Figure 3(a)) to March (Figure 3(c)) and June (Figure 3(f)) to September (Figure 3(i)), this increase in biomass burning increases emission of fine-mode aerosols that elevate the values of AE. In Northern and Eastern, the positive AE during dry months is associated with increase burning in agricultural sector while clearing farms in preparation for tilling of land [34].

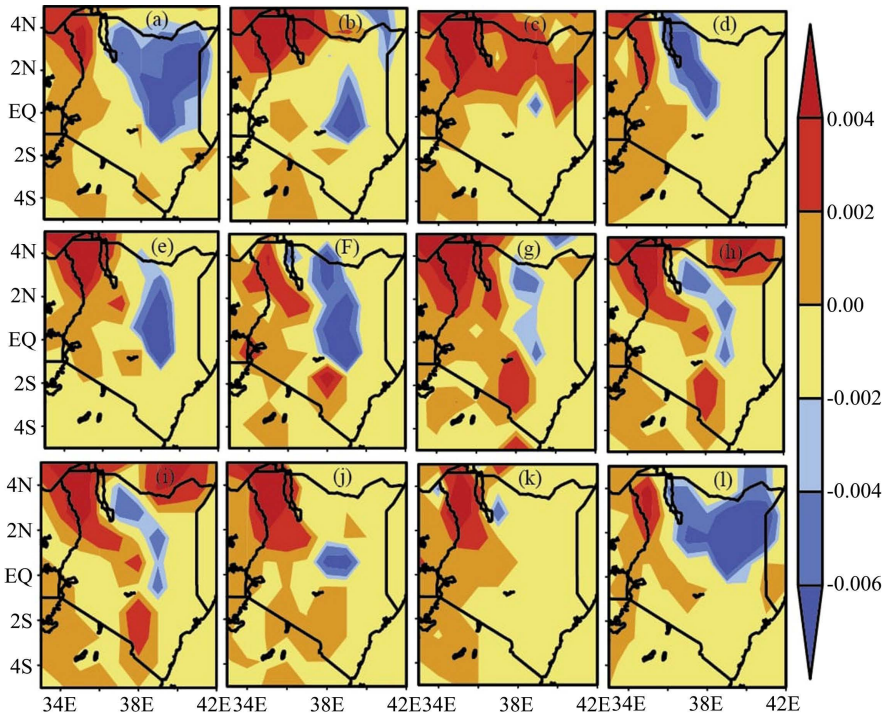

Figure 3. Present time average map trends in angstrom exponent (AE) over Kenya for the period 2005-2022.

Negative trends are dominant in May (**Figure 3(e)**), August (**Figure 3(h)**), September (**Figure 3(i)**), October (**Figure 3(j)**) and December (**Figure 3(l)**) with strong decline in AE trends in Western and Central Kenya. This could be attributed to increase in dust loading. During dry and windy conditions, May (**Figure 3(e)**) to September (**Figure 3(i)**), course-mode desert and semi-arid dust is transported from arid like Northern Kenya, Turkana and Sahel, this results into decrease in AE values [35] Majority of these regions recorded values below 0.00 year^{-1}.

Decreasing in angstrom exponent < −0.002 year^{-1} marked with pale blue and blue, indicating negative anomalies. North Eastern Kenya and the Equator region consistently show negative anomalies more pronounced in January (**Figure 3(a)**), May (**Figure 3(e)**), June (**Figure 3(f)**), October (**Figure 3(j)**) and December (**Figure 3(l)**). This can be attributed to precipitation scavenging, March (**Figure 3(c)**) to May (**Figure 3(e)**) rainy season and October (**Figure 3(j)**) and December (**Figure 3(l)**), precipitation remove fine-mode aerosols more than course-mode particles, this leads to a decrease in AE. During rainy season open burning is limited hence lowering supply of fine-mode aerosol particle from anthropogenic emission [36]. In North eastern, and its neighboring Southern Somalia is semi-arid and arid region, this region experiences soil erosion and dust uplift due to sparse vegetation cover. During dry months, course particles dominate the aerosol load, resulting into decrease in AE within the region. Decline in fine-mode over time results into a decrease in AE trends [35]. North Eastern Kenya has minimal forest and agricultural burning hence low supply of fine-mode particles, this has limited the presence of aerosols that would have increased the AE within the region [34].

Rainfall starts to decline the month of June (**Figure 3(f)**). Dry surface conditions start to emerge again. More pronounced in Eastern and North eastern Kenya, the Tana River basin dust and semi-arid parts of eastern Kenya they become active as a result of wind caused erosion. These course particles are suspended into the atmosphere leading to a decrease in AE with the region. When these particles increase over time and become more frequent, the AE trends become negative [35]. Limited industries in Eastern Kenya hence low pollution density [37].

The coastal region experienced AE close to zero, stable AE. This can be attributed to South-easterly winds; they transport marine aerosols and some course sea salt particles from the Indian Ocean inland. The said aerosols contribute to lower AE, with continuous supply of both course and fine-mode aerosols, from industries and vehicles, they reach a point of dynamic equilibrium thus no variation in AE, doesn't increase nor decrease [38].

December (**Figure 3(l)**) to March (**Figure 3(c)**) there is influence of Northeast monsoon winds which blows from Arabian Peninsula across Somalia into Northern Kenya, these winds carry mineral dust and marine aerosols, which are courser in nature, in turn they load up more course-mode particles in the region while making fine-mode particle less, as result the region record a decrease in AE over

time. Long-range dust particles transported from Arabian Peninsula and Horn of Africa affect Aerosol composition in Northern Kenya [39]. There are evidences of the increase land degradation in North eastern Kenya, overgrazing, deforestation and conflict-driven migration have enhanced dust sources which in turn have contributed to long-term negative AE trends [40].

Most of the regions marked Yellow gave Zero anomalies which implies a stable AE. This can be attributed to consistent in aerosol sources without changing, making AE less likely to change significantly. Very low changes in wind patterns, humidity and precipitation which could have transported aerosols to or from other regions. Low anthropogenic activities which include low industrial growth or urbanization that could have introduced new aerosols into the atmosphere. Little change in rainfall rate or temperature could have affected changes in AE [41]. Dominating negative anomalies were evidence near Somalia April (**Figure 3(d)**) and November (**Figure 3(k)**). There has been decrease in the angstrom exponent over time in Central and Eastern Kenya. Increase in angstrom exponents a positive trend region around the North.

3.3. Trends in Single Scattering Albedo (SSA)

For January (**Figure 4(a)**), February (**Figure 4(b)**) and March (**Figure 4(c)**) exhibit a predominantly negative trend in majority of the region < −0.0006 year^{-1} a smaller region in Western and Nyanza region recorded SSA > −0.0006 year^{-1} but <−0.0002 year^{-1} this shows a decrease in SSA this could be attributed to indicator of an increase in absorbing aerosols which may include black carbon (BC) and Mineral dust. BC is a strong light absorber. Major sources include incomplete combustion of fuel, wildfire and diesel engine. BC absorbs more solar radiation hence reducing SSA [42]. Northern part shows a very large negative trend in SSA of <−0.0014 year^{-1}. This can be attributed to global circulation and jet stream changes, shift in global wind circulation pattern, they transport dust and smoke from other regions and contribute to decrease in SSA [43]. North Rift in (**Figure 4c**) shows at least a positive trend as one moves towards Sudan Boarder, though it's less than 0.0002 year^{-1}. This can be attributed to changes in prevailing wind patterns; North easterly trade winds dominate, transporting aerosols towards the Indian Ocean hence a slight increase in SSA within the region [38].

April (**Figure 4(d)**) experienced a mixed up of positive and negative trend. Eastern and North eastern > −0.0002 year^{-1}, some areas < −0.0002 year^{-1}, other smaller area > 0.0002 year^{-1}. Coastal region less than −0.0006 year^{-1}. Rift valley, Central Kenya, Nairobi, experienced both positive and negative trend less than −0.0006 year^{-1}. This can be attributed to increase in anthropogenic fine aerosol sources, April involves a lot of activities which include land preparation due to shift in climate patterns, Industrial activities, emission of a lot of smoke into the atmosphere [37]. Nyanza and Western Kenya experienced an increase in SSA > 0.0002 year^{-1} attributed to onset of heavy rain, low biomass burning in open air, with less emission of smoke fine-mode aerosols which would have caused a change in SSA

[37].

May (**Figure 4(e)**), June (**Figure 4(f)**), July (**Figure 4(j)**), and November (**Figure 4(k)**), these months experienced an increase in SSA of >−0.0002 year^{-1} in majority of the regions. In June, the rainfall begins to reduce, dry surface conditions re-emerge, especially in eastern and Northeastern, biomass burning in open air increase, smoke transported by wind from other neighboring regions. Dust in Tana River basin and semi-arid and arid regions like Turkana and parts of eastern and northeastern become more active, this results into decrease in SSA within majority of the areas [35]. Negative trend was also dominant especially in Rift Valley (**Figure 4(e)**) and (**Figure 4(g)**), a smaller region in North Rift showed a greater increase in SSA trend > 0.0002 year^{-1} and also in Eastern Kenya with values close to 0.0004 year^{-1}. This can be attributed to Eastern and North Eastern area which have little forest cover, these areas are semi-arid and arid thus less biomass burning in agricultural and preparation, they also lack more established industries that would have contributed to industrial pollution. Urbanization is very low hence Black carbon emission in incomplete combustion of fossil fuel and diesel burning is limited in these regions due to sparse population [34].

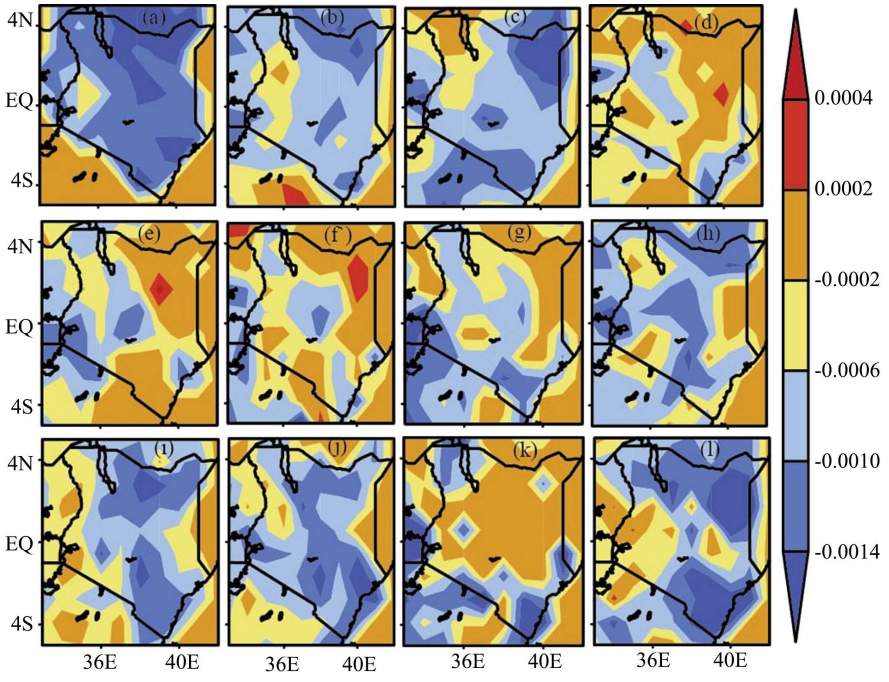

Figure 4. Present time average map for single scattering albedo (SSA) over Kenya for each month from January to December during the period 2005-2022.

August (**Figure 4(h)**), larger part of Eastern showed a decrease in SSA of <−0.0010 year^{-1}, this can be attributed to during August part of the dry season in these regions experience wildfire and agricultural burning, they lead to emission of absorbing aerosols which lower SSA [44]. North Eastern towards Somalia border, SSA increased with values > −0.0002 year^{-1}, Northern part values are less than −0.0006 year^{-1} northeastern Kenya neighbour arid zones like Horn of Africa and

the Sahel, they are major sources of mineral dust. During August wind patterns enhances dust transportation [35]. North rift, south rift, Nairobi and Central Kenya experienced an increase in SSA of greater than −0.0002 year^{-1}. This can be attributed to decline in urban emission, less biomass burning, August, there is heavy downpour in these regions hence less BC emission due to incomplete combustion [37]. Western and Nyanza experienced a decrease of less than −0.0010 year^{-1}. August in western marks the dry season, post-harvest periods often involve burning of crop residues, there is a lot of BC emission during this process [45]. Vehicle emission, charcoal burning and diesel combustion have increased due to growth of Kisumu and Kakamega Towns, they contribute to absorbing aerosols into the atmosphere [46].

September (**Figure 4(i)**) Western and Nyanza experienced an increase in SSA greater than −0.0006 year^{-1}, with some areas around Lake Victoria with SSA close to 0.0002 year^{-1}. September is within the short rain season, there is evidence of wet-scattering aerosols. With increase in rainfall, BC are removed and dust through wet deposit, hence more scattering aerosols such as sulphate and organic matters are left behind in the atmosphere [47]. Sea air masses inflow from Lake Victoria which carry cleaner air, reducing concentration of absorbing aerosols [48]. The SSA trends start to decrease from North Rift towards South Rift, from −0.0002 year^{-1} to −0.0006 year^{-1} in some areas in south rift. Coastal region also recorded a larger decrease in SSA with values less than −0.0010 year^{-1} and −0.0014 year^{-1} some parts of North Eastern, there was a decrease in trend < −0.0002 year^{-1} as one moves towards Somalia border. Eastern and Nairobi, SSA decreased in some parts with values < −0.0010 year^{-1}. This can be attributed to biomass burning in the Horn of Africa and Northern Kenya, cross boarder emission, Sudan, Somalia, Ethiopia, dust emission transport from Garissa, Marsabit, Wajir which contain iron oxides, best absorb radiation hence low SSA [35]. Nairobi experiences strong urban and industrial pollution, a lot of soot and Carbon emitted from vehicle, generators, industries and biomass use such as charcoal [46].

October (**Figure 4(j)**) Western and Nyanza decrease of <−0.0010 year^{-1}, Rift Valley, the North rift experienced decreasing trend of <−0.0006 year^{-1}, with some areas towards Uganda border with decreasing trend of <−0.0002 year^{-1}. Central Kenya, Nairobi recorded decreasing trend of <−0.0010 year^{-1}. Region around the equator negative anomalies of <−0.0002 year^{-1} and <−0.0010 year^{-1} in some areas. Eastern decreasing of <−0.0010 year^{-1}, North Eastern < −0.0006 year^{-1} and values > −0.0002 year^{-1} as one moves towards Somalia boarder. Coastal negative anomalies of <−0.0006 year^{-1} and <−0.0014 year^{-1} in some areas. These can be attributed to reduced rainfall in these regions, lowering wet deposition of absorbing aerosols, which allow them to persist in the atmosphere hence reduction in SSA [49]. October there is very weak precipitation hence poor aerosol scavenging in Eastern, North Eastern and Coastal Kenya, a lower SSA [10].

November (**Figure 4(k)**) Western and Nyanza region < −0.0010 year^{-1}, North rift towards Sudan < −0.0014 year^{-1} and <−0.0006 year^{-1} around lake Turkana.

Attributed to increase in dust emission from arid and semi-arid like Turkana, parts of Eastern and North Eastern. Rift valley leads in mineral dust which affect SSA [35]. South rift < −0.0010 year^{-1}. Nairobi and Central Kenya, majority of areas SSA increase to >−0.002 year^{-1} up to values of 0.0002 year^{-1} positive anomalies attributed to, equator and central highlands are wet during November, rain removes BC and dust from the atmosphere hence increase in scattering [10]. Area around the equator increasing trend > −0.0002 year^{-1} tending to zero anomalies. Eastern recorded a decrease of <−0.0002 year^{-1}. North eastern there was an increase with decrease in some parts with <−0.0014 year^{-1}. Coastal region < −0.0010 year^{-1} and <−0.0006 year^{-1} in some area, decreasing trend attributed to long range transport of absorbing aerosols from Horn of Africa and Southern Africa due to change in the direction of wind [50].

December (**Figure 4(l)**) Western, Nyanza and some parts of Rift valley, Nairobi and central and area around the Equator SSA decreased with values less than −0.0002 year^{-1} to −0.0006 year^{-1}. North Rift decreases less than −0.0010 year^{-1} around Lake Turkana towards Sudan −0.0006 year^{-1}. Eastern, North parts less than −0.0010 year^{-1}. North eastern less than −0.0010 year^{-1} and −0.0014 year^{-1} some parts increase of greater than 0.0002 year^{-1}. Central Region less than −0.0010 year^{-1} but greater than −0.0014 year^{-1}. December post-harvest practices are more in Western Kenya, Rift valley, and Central Kenya, burning of maize residue, sugar residue and general clearing land; releases a lot of smoke into the atmosphere, this smoke contain a lot of absorbing aerosols than scattering, as a result the ratio of absorbing to scattering is greater than 1 which makes SSA to decrease [51]. There is very little or no short rain at all wet deposits of BC which remain into the atmosphere [10]. Travel, cooking and industrial activities increase in urban Centers such as Nairobi, Nakuru, Mombasa, Eldoret and Kisumu during month of December, this increased emission of diesel soot, charcoal smoke, which are sources of absorbing aerosols [46].

3.4. Trends Analysis in Average Time Rainfall Rates (RR)

Positive values show an increasing trend in rainfall rate while negative values represent a decreasing trend in rainfall rate. January to December, majority of region experienced a decreasing trend in RR with values < −0.01 year^{-1}. January (**Figure 5(a)**) The entire country experienced a negative trend with values < −0.01 year^{-1} all values trend is below zero indicating a very serious negative anomalies within the country. January is within the dry season of the year. A small area within the rift valley recorded a slightly higher RR trend greater than −0.01 year^{-1} though the values are also within the negative trends.

RR starts showing as slight increase from Lake Victoria region, western, and some part of South rift February (**Figure 5(b)**), March (**Figure 5(c)**), there is a slight increase in RR within the country more specific within, rift valley, Nairobi and some parts of Western Region, though its slightly below zero. It's a clear indicator that the rainfall has constantly decreased within the regions. The decline

in RR within the country for major seasons March (**Figure 5(c)**) to May (**Figure 5(e)**) long rain season, in most parts of western Kenya, especially central and western regions, with peak in April (**Figure 5(d)**), the cool dry season June (**Figure 5(f)**) to August (**Figure 5(h)**) with peak in July (**Figure 5(g)**). the short rains October (**Figure 5(j)**) to December (**Figure 5(l)**) with peak in November (**Figure 5(k)**). The hot dry season January (**Figure 5(a)**) to February (**Figure 5(b)**) with peak in February very hot in lowland areas like Turkana, Garissa and coastal region recording the highest SAT. This decline can be attributed to climate change, the country is experiencing global warming which has disrupted traditional rainfall patterns across majority of countries within East Africa. This has led to more frequent and prolonged droughts. Warmer SAT increases evaporation rates, reducing soil moisture and suppressing rainfall formation [52].

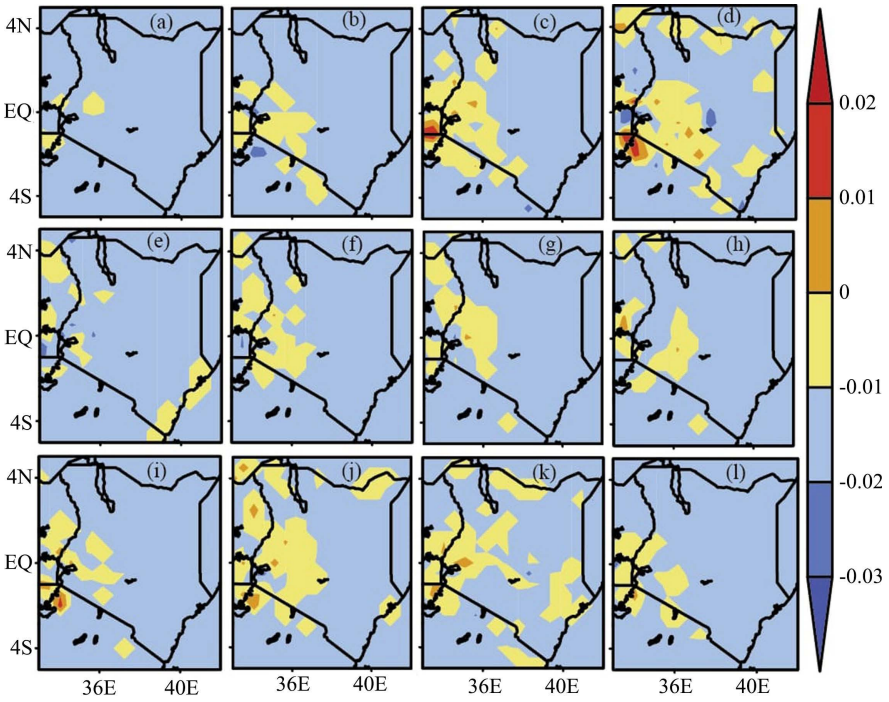

Figure 5. Present time average map for rainfall rates deg. [TRMM] over 2000-2022.

There have been sea surface temperature anomalies. Variabilities in IOD and ENSO have altered rainfall distribution. Negative IOD are characterized by prolonged dry season while positive IOD are characterized by floods, which may include flash floods [53]. La Nina episode shifts moisture away from the region hence suppressing rainfall, El Nino and La Nina events have become erratic. El Nino increases rainfall patterns have been unpredictable. La Nina events of 2010-2011 and 2020-2022 have been associated with droughts in the country [10].

Kenya is becoming increasingly dry due to climate impacts within the region [54]. There are so many cases of changes in land use program and also evidences of deforestation. For instance, Mau Forest complex, by evading the forest to create room for settlement, the green cover was greatly reduced. This reduced evapo-

transpiration and disrupted local rainfall generation. Less evapotranspiration means less local cloud formation and rainfall. Area around Mau Forest, such as Nakuru, Kericho, Bomet and Narok have reported decline rainfall trends [55]. The conversion of forests and wetlands into farmland and settlements alters regional hydrology. It also disrupts hydrological cycle. Mau Forest played a critical role in feeding Major rivers like Mara, Ewaso Ng'iro and Sondu Miriu, they sustained wetlands, Lake Nakuru, Lake Victoria and Livelihoods. Majority of these rivers are drying up and RR within the region has decreased. Forests act as caron sink and climatic regulator. Its destruction has contributed to increased greenhouse gas emission affecting regional RR dynamics and exacerbating climate change effects in Kenya and East Africa at Large [55].

Degradation of watersheds and wetlands through unsustainable farming which includes monoculture farming, excessive use of chemical fertilizers and pesticides, overgrazing, deforestation for agriculture, improper irrigation practices, tillage and soil mismanagement, burning agricultural residue among others, charcoal burning and wetland encroachment affect water retention and humidity regulation, it further reduces RR [56].

There has been increase in aerosol concentration which includes dust, soot, pollutants from both anthropogenic and natural cause in the atmosphere can suppress cloud formation and RR by affecting cloud microphysics [57]. Increase urbanization and microclimate alterations. Kenya is experiencing rapid urban sprawl in Nairobi, Mombasa, Kisumu, Nakuru and Eldoret. With expansion of cities and towns, vegetation is being cleared to create room for Roads, buildings among many other establishments.

This practice affects local atmospheric dynamics and reduces moisture recycling. Sealing of surface *i.e.*, concrete and tarmac roads, reduces infiltration and local humidity, thus affecting the rainfall within a region [58]. Rapid urban development in cities and towns has changed the surface albedo and heat dynamics, this has disrupted local convection processes essential for rainfall formation [59].

Global circulation and Jet stream have changed. Shifts in global wind circulation patterns, such as the sub-tropical jet stream, delay and weaken rainy seasons [43]. Kenya has experienced degradation of water bodies and wetlands. Shrinking of lake Nakuru, Lake Victoria has led to reduction in localized convection and precipitation [60].

3.5. Trends Analysis Time Averaged Surface Air Temperature (SAT)

January (**Figure 6(a)**) western Kenya, Nyanza region and North eastern Kenya experienced a decrease in SAT of <-0.01 year^{-1} which was a negative anomaly, with regions around the Lake Victoria recording negative trends of <-0.02 year^{-1}. This could be attributed to El Nino-Southern Oscillation (ENSO) a climate pattern that causes fluctuation in temperature [61]. North rift experienced an increase in SAT of >0.02 especially as one moves towards lake Turkana, Nairobi, Central and parts of South rift also experienced an increase in SAT, this could be

attributed to greenhouse gas emission, which may include burning of fossil fuel which contribute to accumulation of Carbon (iv) oxide which is a greenhouse gas that results into increase in temperature over a particular region [62].

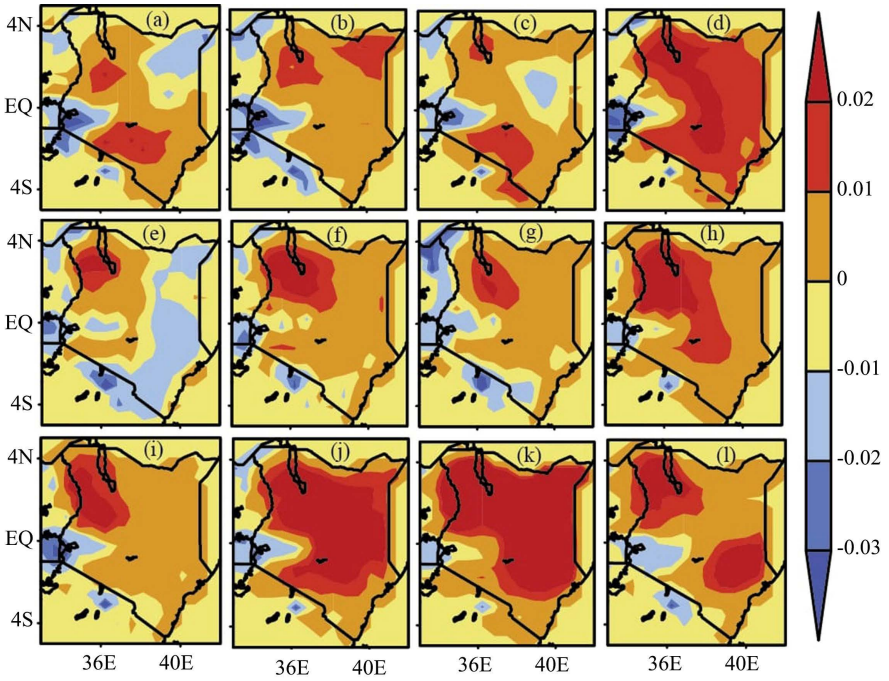

Figure 6. Present time average map for surface air temperature deg. [MODIS-Terra] over 2000-2022.

Majority of areas within Eastern, Rift Valley, Coastal and Northeastern experienced temperature trends above Zero but less than 0.01 which indicated a positive anomaly. This could be attributed to the fact that January is within the dry season in Kenya, greenhouse effect is also a factor transport and industrial processes releases Carbon (iv) oxide which accumulate in the atmosphere triggering the temperature, hence fluctuation [63]. Small areas within the North Eastern and rift valley experienced a negative anomaly below zero but less than −0.01, indicator of a negative anomaly since all values are negatives. This could be attributed to evidence of volcanic eruption and change in Ocean current which might have caused a negative change in SAT [61].

February (**Figure 6(b)**), majority of the region experienced temperature trends above zero. With values less than 0.001 year^{-1} North Eastern and North rift especially around lake Turkana recorded values greater than +0.001 year^{-1} this can be attributed to increase in deforestation, forest play a vital role in climate change and with the current change in land usage, clearing forests to create room for settlement, logging, high demand for wood fuel have left a very small area for forest coverage. Kenya lost 400 kha of tree cover, about 12% of the 2000 tree cover area and 200 Mt of CO2e emission 2001-2024 [64].

March (**Figure 6(c)**) Rift valley, Coastal region, Eastern, North-eastern majority of the area recorded increase in temperature trends above zero. South rift, Nai-

robi, Central parts of Eastern and around Lake Turkana, recorded trends value less than 0.01 year^{-1}, the value is positive above zero. This could be attributed to heatwaves frequency and severity in North Eastern counties, Garissa, Mandera and Wajir. These regions have higher albedo which makes it more sensitive to radiative forcing [65]. Wajir and Garissa are expanding introducing urban heat island effect. Nairobi with so many buildings having covered a larger area, concrete, asphalt and buildings traps heat more than natural land cover thus causing an increase in temperature trends within the region [66] [67]. Lake Victoria experienced trends of −0.02 year^{-1}. This could be attributed to enhanced evaporation from Lake Surface cooling effect due to constant evaporation. Expansion of wetlands, reforestation initiative in Lake Victoria basin cloud have increased evapotranspiration localizing cooling [68].

April (**Figure 6(d)**), the whole country experienced an increase in SAT of greater than +0.01 year^{-1} with some regions recording values above +0.02 year^{-1}. Evidence of high increase in SAT within the country. This can be attributed to increase in greenhouse gas emissions. Methane from livestock and rice cultivation, increase in motor transport within the country, high investment in establishment of industries, there has been high emission of Carbon (iv) oxide which cannot be reduced due to evidence of reduced green cover as a result of deforestation [62] [63]. Around Lake Victoria values decreased from −0.01 year^{-1} to less than −0.02 year^{-1}. This could be attributed to data or measurement factors. There could be change in satellite sensor, calibration. Station relocation or data homogenization methods also, could be as a result of lake breeze effect, the diurnal lake-land breeze system and changing wind patterns [68].

May (**Figure 6(e)**) North Rift towards Sudan around Lake Turkana values > +0.01 year^{-1}. Majority of Rift valley, parts of Nyanza, Eastern, Nairobi, Central and around the equator experienced increase in SAT. This can be attributed to introducing aerosols that warm the nights by increasing downward longwave radiation estimated about 6 - 13 Wm^{-2}. They modify radiation balance and cloud formation adding to regional warming [69]. ENSO and Indian Ocean Dipole (IOD) significantly influence East Africa climate, positive IOD and El Nino are associated with high SAT [70]. ENSO links with dust transport and aerosol variability indirectly affecting SAT [71]. The coastal region, North eastern and parts of eastern recorded a negative anomaly in SAT < −0.01 year^{-1}. This could be attributed to change in wind pattern transporting aerosols from distant sources to the Kenya Somalia border, this could have resulted in changes in SAT [33]. Aerosols modify radiation balance and cloud formation adding to regional warming [69].

June (**Figure 6(f)**) Majority of regions experienced increase in temperature close to +0.01 year^{-1}. This could be attributed to shifting in climate zones, hotter, drier conditions in Turkana are spreading southwards. This is evidence in increased heat stress in Baringo, Samburu and even parts of Central Kenya [72]-[74]. Around lake Turkana, temperature increased with larger values greater than

+0.01 year^{-1} with values up to +0.02 year^{-1} trends. Smaller area within North-eastern temperature less than 0.02. Turkana is semi-arid region, hence sensitive to small changes in climate, making warming effect more noticeable. It lies in a dry, desert-like region with very low vegetation cover, this makes it heat up faster, bare soils absorb and retain more heat [74] [75].

July (**Figure 6(g)**) Majority of regions increased in SAT up to +0.01 year^{-1} North rift around lake Turkana valued increased above +0.01 year^{-1}. Parts of rift valley SAT increase with values above −0.01 year^{-1}. This could be attributed to infrastructure projects and human settlement, for instance Gibe III dam in Ethiopia affect Lake Turkana in flow. Urbanization around the lake and nearby region like Lodwar has created urban heat island. Overgrazing, charcoal burning lead to lose of vegetation cover hence reducing natural cooling increasing local temperature [72].

August (**Figure 6(h)**) Temperature increased from Turkana towards Eastern, Nairobi, Central and majority of North Rift greater than 0.01 year^{-1} and with some areas with greater than 0.02 year^{-1}. Majority of the regions experienced SAT increase, a positive anomaly. This could be attributed to shifting climate zones, Shifting Northwards. High temperature spreads downwards due to changes in wind patterns. Hence increase in temperature in Regions like Samburu, Baringo and Laikipia [75]. Increase in anthropogenic heat emission due to increase in urbanization, buildings retain a lot of heat that they are unable to release hence, increased SAT within Nairobi [68].

September (**Figure 6(i)**) Majority of parts of the Country experienced high rise in SAT up to 0.01 year^{-1}. North rift experienced high increase of SAT up to 0.02 year^{-1}. This can be attributed to more frequent and intense droughts. Climate change is exacerbating droughts in Kenya, making them more frequent and severe. There has been a decrease in rainfall and increased evaporation thus reducing hydropower capacity leading to increase in SAT throughout the country, spreading to other regions within [68].

October (**Figure 6(j)**) There was evidence of increase in SAT of majority of the region within the country. High temperature trend of >0.01 year^{-1} with many regions having values > 0.02 year^{-1}. Coastal Region experienced an increase of up to +0.01 year^{-1}. All this could be attributed to a shift climate zones, deforestation, land use change, logging and demand for firewood [63]. Region around Lake Victoria experienced a decrease in SAT. attributed to enhanced evaporation from Lake surface, cooling effect due to constant evaporation [68].

November (**Figure 6(k)**) Very high temperature trends were experienced almost in the entire country. Only Coastal and some parts of south rift experienced values of 0.01 year^{-1}, which is still positive anomalies. Lake Victoria continued recording negative trend. High temperatures within the entire country can be attributed to season, November is within the dry season. Land use practice would have changed, less rainfall patterns, dry lands absorbing a lot of heat radiation from the sun, high albedo and increased AOD hence retaining heat on earth sur-

face [33] [32] [31].

December (**Figure 6(l)**) Majority of the region experienced increased values in SAT trend, ranging from 0.01 year^{-1} to 0.02 year^{-1} a positive trend. This can be attributed to declining rainfall and increased evaporation, higher evaporation in arid and semi-arid regions leading to drop of lake level hence contributing to regional warming. Lack of enough vegetation cover makes the ground heat up faster, bare soil absorbs and retains more heat [72]-[75]. Lake Victoria Maintain a decrease throughout the year despite December being within the dry season of the year.

4. Summary and Conclusions

1) AOD decreased in most parts of the country, there is decrease in aerosol loading, influenced by Biomass burning, changes in wind pattern hence migration of dust from one region to another, and changes in rainfall rates hence leaving ground very dry with loose dry matters. Northern Kenya and eastern showed high AOD values due to the nature of the region, arid and semi-arid, also there was effect of Sahara and Dust from the Horn of Africa including Sahel. Western, Central and Nairobi experienced moderate AOD with fluctuating trends due to changes of rainfall season, variation from long to short rains. Coastal experienced lower AOD due to influence of IOD and ENSO inland. This suggests that change in biomass burning and wind patterns influence AOD.

2) Kenya experienced moderate to high AE which was a mixture of fine-mode particles and course-mode particles, shift in climate pattern from north to south affected the stability of AE which varied from moderate, high and low depending on the nature of particles that were available in the atmosphere. When Biomass burning fine-mode aerosols were more dominance hence increase in AE. AE values vary with size of particles present in atmosphere.

3) SSA decreased with increase in absorbing aerosols which included BC, biomass burning, diesel, fossil fuel incomplete combustion. SSA decreased more during dry season due to increase in biomass burning releasing more smoke into the atmosphere. Changes in wind direction led to transportation of long-range absorbing aerosols from distance regions such as Horn of Africa, Sahel, Sahara Desert which affect SSA. Wind direction influences SSA.

4) SSA increases during wet season, there is decline in absorbing aerosol and results into increase in scattering aerosols into the atmosphere. Rain washes out the fine-mode aerosols from the atmosphere leaving course-mode aerosols which have good scattering properties hence leading to an increase in SSA.

5) Rainfall rate in Kenya 2000-2022 showed high interannual variability with almost zero consistent long-term trend, attributed to influence of regional climate drivers such as ENSO and IOD. The SAT exhibited a general warming trend, indicating rising regional temperature linked to global climate change.

6) AOP in Kenya showed a noticeable association with climate variables. High aerosol loading corresponded with reduced rainfall and increased temperatures. Aerosol influences regional climate.

7) The study limitation arose from the course spatial resolution of satellite data, which could have localized variations in aerosol and climate behavior across Kenya. HMM assumptions *i.e.*, Markov property, stationarity of transition probabilities, and predefined emission distributions and simplifying complex atmospheric processes such as extreme events may limit the model's ability to fully capture the dynamics of aerosol-climate associations.

Acknowledgements

I appreciate my supervisors Prof. John W. Makokha and Dr. Geoffrey W. Khamala for their support to make my study process successful. Secondly my sincere gratitude to the NASA and Giovanni online analysis and visualization system for providing and processing MODIS, MERRA-2 data used in this study. Lastly to the Almighty God for his unfailing love and His favor through this process. To God be glory and honor.

Conflicts of Interest

The authors have no conflict of interest whatsoever.

References

[1] Khamala, G.W., Odhiambo, J.O. and Makokha, J.W. (2018) Seasonal Variability in Aerosol Microphysical Properties over Selected Rural, Urban and Maritime Sites in Kenya. *Open Access Library Journal*, **5**, 1-20. https://doi.org/10.4236/oalib.1104821

[2] Khamala, G.W., Makokha, J.W., Boiyo, R. and Kumar, K.R. (2022) Long-Term Climatology and Spatial Trends of Absorption, Scattering, and Total Aerosol Optical Depths over East Africa during 2001-2019. *Environmental Science and Pollution Research*, **29**, 61283-61297. https://doi.org/10.1007/s11356-022-20022-6

[3] Kaufman, Y.J., Tanré, D. and Boucher, O. (2002) A Satellite View of Aerosols in the Climate System. *Nature*, **419**, 215-223. https://doi.org/10.1038/nature01091

[4] Garland, R.M., Yang, H., Schmid, O., Rose, D., Nowak, A., Achtert, P., *et al.* (2008) Aerosol Optical Properties in a Rural Environment near the Mega-City Guangzhou, China: Implications for Regional Air Pollution, Radiative Forcing and Remote Sensing. *Atmospheric Chemistry and Physics*, **8**, 5161-5186. https://doi.org/10.5194/acp-8-5161-2008

[5] Cheng, F., Li, W., Zhou, Y., Shen, J., Wu, Z., Liu, G., *et al.* (2012) ad-metSAR: A Comprehensive Source and Free Tool for Assessment of Chemical ADMET Properties. *Journal of Chemical Information and Modeling*, **52**, 3099-3105. https://doi.org/10.1021/ci300367a

[6] Li, L., Chen, Z., Liu, P. and Zhang, Y. (2022) Direct Measurement of pH Evolution in Aerosol Microdroplets Undergoing Ammonium Depletion: A Surface-Enhanced Raman Spectroscopy Approach. *Environmental Science & Technology*, **56**, 6274-6281. https://doi.org/10.1021/acs.est.1c08626

[7] Khamala, G.W., Makokha, J.W., Boiyo, R. and Kumar, K.R. (2023) Spatiotemporal Analysis of Absorbing Aerosols and Radiative Forcing over Environmentally Distinct Stations in East Africa during 2001-2018. *Science of the Total Environment*, **864**, Article ID: 161041. https://doi.org/10.1016/j.scitotenv.2022.161041

[8] Shilenje, Z.W., Maloba, S. and Ongoma, V. (2022) A Review on Household Air Pol-

lution and Biomass Use over Kenya. *Frontiers in Environmental Science*, **10**, Article ID: 996038. https://doi.org/10.3389/fenvs.2022.996038

[9] Otieno, V.O. and Anyah, R.O. (2012) CMIP5 Simulated Climate Conditions of the Greater Horn of Africa (GHA). Part 1: Contemporary Climate. *Climate Dynamics*, **41**, 2081-2097. https://doi.org/10.1007/s00382-012-1549-z

[10] Nicholson, S.E. (2017) Climate and Climatic Variability of Rainfall over Eastern Africa. *Reviews of Geophysics*, **55**, 590-635. https://doi.org/10.1002/2016rg000544

[11] Holben, B.N., Eck, T.F., Slutsker, I., Tanré, D., Buis, J.P., Setzer, A., *et al.* (1998) AERONET—A Federated Instrument Network and Data Archive for Aerosol Characterization. *Remote Sensing of Environment*, **66**, 1-16. https://doi.org/10.1016/s0034-4257(98)00031-5

[12] Rabiner, L. and Juang, B. (1986) An Introduction to Hidden Markov Models. *IEEE ASSP Magazine*, **3**, 4-16.

[13] Kandanaarachchi, S. (2022) Unsupervised Anomaly Detection Ensembles Using Item Response Theory. *Information Sciences*, **587**, 142-163. https://doi.org/10.1016/j.ins.2021.12.042

[14] Eddy, S.R. (2004) What Is a Hidden Markov Model? *Nature Biotechnology*, **22**, 1315-1316. https://doi.org/10.1038/nbt1004-1315

[15] Kreymer, S., Singer, A. and Bendory, T. (2022) An Approximate Expectation-Maximization for Two-Dimensional Multi-Target Detection. *IEEE Signal Processing Letters*, **29**, 1087-1091. https://doi.org/10.1109/lsp.2022.3167335

[16] Anderson, T.L., Masonis, S.J., Covert, D.S., Ahlquist, N.C., Howell, S.G., Clarke, A.D., *et al.* (2003) Variability of Aerosol Optical Properties Derived from *in Situ* Aircraft Measurements during ACE-Asia. *Journal of Geophysical Research*: *Atmospheres*, **108**, Article No. 8647. https://doi.org/10.1029/2002jd003247

[17] Ongoma, V. and Chen, H. (2016) Temporal and Spatial Variability of Temperature and Precipitation over East Africa from 1951 to 2010. *Meteorology and Atmospheric Physics*, **129**, 131-144. https://doi.org/10.1007/s00703-016-0462-0

[18] Makokha, J.W. and Angeyo, H.K. (2013) Investigation of Radiative Characteristics of the Kenyan Atmosphere Due to Aerosols Using Sun Spectrophotometry Measurements and the COART Model. *Aerosol and Air Quality Research*, **13**, 201-208. https://doi.org/10.4209/aaqr.2012.06.0146

[19] Boiyo, R., Kumar, K.R., Zhao, T. and Bao, Y. (2017) Climatological Analysis of Aerosol Optical Properties over East Africa Observed from Space-Borne Sensors during 2001-2015. *Atmospheric Environment*, **152**, 298-313. https://doi.org/10.1016/j.atmosenv.2016.12.050

[20] Levy, R.C., Remer, L.A., Mattoo, S., Vermote, E.F. and Kaufman, Y.J. (2007) Second-generation Operational Algorithm: Retrieval of Aerosol Properties over Land from Inversion of Moderate Resolution Imaging Spectroradiometer Spectral Reflectance. *Journal of Geophysical Research*: *Atmospheres*, **112**, D13211. https://doi.org/10.1029/2006jd007811

[21] Hsu, C.W. and Kuo, T.H. (2003) 6-Bit 500 MHz Flash A/D Converter with New Design Techniques. *IEE Proceedings—Circuits*, *Devices and Systems*, **150**, 460-464. https://doi.org/10.1049/ip-cds:20030604

[22] Hsu, T.Y., Ke, H.R. and Yang, W.P. (2006) Knowledge-Based Mobile Learning Framework for Museums. *The Electronic Library*, **24**, 635-648. https://doi.org/10.1108/02640470610707240

[23] Levy, R.C., Remer, L.A., Kleidman, R.G., Mattoo, S., Ichoku, C., Kahn, R., *et al.* (2010)

Global Evaluation of the Collection 5 MODIS Dark-Target Aerosol Products over Land. *Atmospheric Chemistry and Physics*, **10**, 10399-10420. https://doi.org/10.5194/acp-10-10399-2010

[24] Mathur, B. (2022) Predicting Atmospheric Variables in the MERRA-2 Database Using Neural Networks. 2022 *International Conference on Emerging Techniques in Computational Intelligence* (*ICETCI*), Hyderabad, 25-27 August 2022, 125-131. https://doi.org/10.1109/icetci55171.2022.9921371

[25] Todling, R. and El Akkraoui, A. (2018) The GMAO Hybrid Ensemble-Variational Atmospheric Data Assimilation System: Version 2.0 (No. GSFC-E-DAA-TN54363).

[26] Cullather, R. and Bosilovich, M. (2017) Climate Data Guide-Modern Era Retrospective Analysis for Research and Applications, Version 2 (MERRA-2) (No. GSFC-E-DAA-TN48293).

[27] Theon, J.S. (1994) The Tropical Rainfall Measuring Mission (TRMM). *Advances in Space Research*, **14**, 159-165. https://doi.org/10.1016/0273-1177(94)90210-0

[28] Simpson, J. (1988) A Satellite Mission to Measure Tropical Rainfall. Report of the Science Steering Group. NASA/GSFC.

[29] Chiu, L.S., Shin, D. and Kwiatkowski, J. (2006) Surface Rain Rates from Tropical Rainfall Measuring Mission Satellite Algorithms. In: Qu, J.J., *et al.*, Eds., *Earth Science Satellite Remote Sensing*: *Vol.* 1: *Science and Instruments*, Springer, 317-336. https://doi.org/10.1007/978-3-540-37293-6_17

[30] Kimani, W., Gatebe, C. and Kinuthia, J. (2021) Variability and Trends of Aerosol Optical Depth and Climate Variables over East Africa. *Atmospheric Environment*, **248**, Article ID: 118210.

[31] Mutama, P.M., Makokha, J.W., Kelonye, F.B. and Khamala, G.W. (2024) Spatial-Temporal Assessment of Changes in Aerosol Optical Properties Pre, during, and Post COVID-19 Lockdowns over Kenya, East Africa. *Open Access Library Journal*, **11**, 1-14. https://doi.org/10.4236/oalib.1111223

[32] Gupta, G., Venkat Ratnam, M., Madhavan, B.L. and Narayanamurthy, C.S. (2022) Long-Term Trends in Aerosol Optical Depth Obtained across the Globe Using Multi-Satellite Measurements. *Atmospheric Environment*, **273**, Article ID: 118953. https://doi.org/10.1016/j.atmosenv.2022.118953

[33] Stephens, G.L., Shiro, K.A., Hakuba, M.Z., Takahashi, H., Pilewskie, J.A., Andrews, T., *et al.* (2024) Tropical Deep Convection, Cloud Feedbacks and Climate Sensitivity. *Surveys in Geophysics*, **45**, 1903-1931. https://doi.org/10.1007/s10712-024-09831-1

[34] Eck, T.F., Holben, B.N., Sinyuk, A., Pinker, R.T., Goloub, P., Chen, H., *et al.* (2010) Climatological Aspects of the Optical Properties of Fine/Coarse Mode Aerosol Mixtures. *Journal of Geophysical Research*: *Atmospheres*, **115**. https://doi.org/10.1029/2010JD014002

[35] Engelstaedter, S., Tegen, I. and Washington, R. (2006) North African Dust Emissions and Transport. *Earth-Science Reviews*, **79**, 73-100. https://doi.org/10.1016/j.earscirev.2006.06.004

[36] Kang, N., Kim, Y.J., Kim, H. and Kim, K.C. (2016) Wet Scavenging of Aerosols and Their Chemical Components by Summertime Rainfall in an Urban Area of Korea. *Atmospheric Environment*, **127**, 13-22.

[37] Gatari, M.J. and Boman, J. (2003) Black Carbon and Total Carbon Measurements at Urban and Rural Sites in Kenya, East Africa. *Atmospheric Environment*, **37**, 1149-1154. https://doi.org/10.1016/s1352-2310(02)01001-4

[38] Prospero, J.M. and Lamb, P.J. (2003) African Droughts and Dust Transport to the

Caribbean. *Bulletin of the American Meteorological Society*, **84**, 873-883. https://www.science.org/doi/10.1126/science.1089915

[39] Prospero, J.M. and Nees, R.T. (1986) Impact of the North African Drought and El Niño on Mineral Dust in the Barbados Trade Winds. *Nature*, **320**, 735-738. https://doi.org/10.1038/320735a0

[40] Anyah, R.O. and Qiu, W. (2012) Characteristic Trends in Land Surface Temperature and Vegetation over Africa. *Climate Research*, **52**, 77-91.

[41] Eck, T.F., Holben, B.N., Reid, J.S., Dubovik, O., Smirnov, A., O'neill, N.T. and Kinne, S. (1999) Wavelength Dependence of the Optical Depth of Biomass Burning, Urban, and Desert Dust Aerosols. *Journal of Geophysical Research*: *Atmospheres*, **104**, 31333-31349. https://doi.org/10.1029/1999JD900923

[42] Kirago, L., Gatari, M.J., Gustafsson, Ö. and Andersson, A. (2022) Black Carbon Emissions from Traffic Contribute Substantially to Air Pollution in Nairobi, Kenya. *Communications Earth & Environment*, **3**, Article No. 74. https://doi.org/10.1038/s43247-022-00400-1

[43] Rowell, D.P., Booth, B.B.B., Nicholson, S.E. and Good, P. (2015) Reconciling Past and Future Rainfall Trends over East Africa. *Journal of Climate*, **28**, 9768-9788. https://doi.org/10.1175/jcli-d-15-0140.1

[44] Liousse, C., Assamoi, E., Criqui, P., Granier, C. and Rosset, R. (2014) Explosive Growth in African Combustion Emissions from 2005 to 2030. *Environmental Research Letters*, **9**, Article ID: 035003. https://doi.org/10.1088/1748-9326/9/3/035003

[45] Wiedinmyer, C., Yokelson, R.J. and Gullett, B.K. (2014) Global Emissions of Trace Gases, Particulate Matter, and Hazardous Air Pollutants from Open Burning of Domestic Waste. *Environmental Science & Technology*, **48**, 9523-9530. https://doi.org/10.1021/es502250z

[46] Kinney (2011) Airborne Particulate Matter in Two Nairobi Neighbourhoods: Concentrations, Composition, and Sources. *Atmospheric Environment*, **45**, 6844-6851.

[47] Andreae, M.O. and Rosenfeld, D. (2008) Aerosol-Cloud-Precipitation Interactions. Part 1. The Nature and Sources of Cloud-Active Aerosols. *Earth-Science Reviews*, **89**, 13-41. https://doi.org/10.1016/j.earscirev.2008.03.001

[48] Makokha, G.L. and Shisanya, C.A. (2010) Trends in Mean Annual Minimum and Maximum near Surface Temperature in Nairobi City, Kenya. *Advances in Meteorology*, **2010**, Article ID: 676041. https://doi.org/10.1155/2010/676041

[49] Jaenicke, R. (2005) Abundance of Common Aerosols in the Troposphere. A Review. *Tellus Bi Chemical and Physical Meteorology*, **51**, 200-216.

[50] Vakkari, V. (2018) Rapid Changes in Biomass Burning Aerosols by Atmospheric Oxidation. *Geophysical Research Letters*, **45**, 4639-4647.

[51] Andreae, M.O. and Merlet, P. (2001) Emission of Trace Gases and Aerosols from Biomass Burning. *Global Biogeochemical Cycles*, **15**, 955-966. https://doi.org/10.1029/2000gb001382

[52] Kikstra, J.S., Nicholls, Z.R.J., Smith, C.J., Lewis, J., Lamboll, R.D., Byers, E., *et al.* (2022) The IPCC Sixth Assessment Report WGIII Climate Assessment of Mitigation Pathways: From Emissions to Global Temperatures. *Geoscientific Model Development*, **15**, 9075-9109. https://doi.org/10.5194/gmd-15-9075-2022

[53] Ummenhofer, C.C., Sen Gupta, A., England, M.H. and Reason, C.J.C. (2009) Contributions of Indian Ocean Sea Surface Temperatures to Enhanced East African Rainfall. *Journal of Climate*, **22**, 993-1013. https://doi.org/10.1175/2008jcli2493.1

[54] Niang, A., Becker, M., Ewert, F., Dieng, I., Gaiser, T., Tanaka, A., *et al.* (2017) Varia-

bility and Determinants of Yields in Rice Production Systems of West Africa. *Field Crops Research*, **207**, 1-12. https://doi.org/10.1016/j.fcr.2017.02.014

[55] Mwangi, H.M., Julich, S., Patil, S.D., McDonald, M.A. and Feger, K. (2016) Relative Contribution of Land Use Change and Climate Variability on Discharge of Upper Mara River, Kenya. *Journal of Hydrology*: *Regional Studies*, **5**, 244-260. https://doi.org/10.1016/j.ejrh.2015.12.059

[56] Crafford, J., Strohmaier, R., Muñoz, P., Oliveira, T.D., Lambrechts, C., Wilkinson, M. and Bosch, J. (2012) The Role and Contribution of Montane Forests and Related Ecosystem Services to the Kenyan Economy. 49.

[57] Acker, J.G. and Leptoukh, G. (2007) Online Analysis Enhances Use of NASA Earth Science Data. *Eos*, *Transactions American Geophysical Union*, **88**, 14-17. https://doi.org/10.1029/2007eo020003

[58] Ndolo, I.J., Nzioka, J.M., Oludhe, C., Ng'ang'a, J.K. and Odingo, R.S. (2018) Influence of Urbanisation on Minimum and Maximum Temperature Characteristics over Nairobi City.

[59] Munyao, M., Siljander, M., Johansson, T., Makokha, G. and Pellikka, P. (2020) Assessment of Human-elephant Conflicts in Multifunctional Landscapes of Taita Taveta County, Kenya. *Global Ecology and Conservation*, **24**, e01382. https://doi.org/10.1016/j.gecco.2020.e01382

[60] Aloo, P.A., Njiru, J., Balirwa, J.S. and Nyamweya, C.S. (2017) Impacts of Nile Perch, *Lates niloticus*, Introduction on the Ecology, Economy and Conservation of Lake Victoria, East Africa. *Lakes & Reservoirs*: *Science*, *Policy and Management for Sustainable Use*, **22**, 320-333. https://doi.org/10.1111/lre.12192

[61] Timmermann, A., An, S., Kug, J., Jin, F., Cai, W., Capotondi, A., *et al.* (2018) El Niño-southern Oscillation Complexity. *Nature*, **559**, 535-545. https://doi.org/10.1038/s41586-018-0252-6

[62] Omambia, A.N., Shemsanga, C. and Li, Y. (2009) Combating Climate Change in Kenya: Efforts, Challenges and Opportunities. *Report and Opinion*, **1**, 12-23.

[63] Marigi, S.N. (2017) Climate Change Vulnerability and Impacts Analysis in Kenya. *American Journal of Climate Change*, **6**, 52-74. https://doi.org/10.4236/ajcc.2017.61004

[64] Araujo, Z., Gusti, M., Wu, Y., Kakai, L., Havlik, P. and Corbeels, M. (2024) Kenya's Perspectives across Climate, Conservation, and Climax+ Conservation Scenarios Using Global Forest Model (G4M).

[65] Cao, J., Zhou, W., Yu, W., Hu, X., Yu, M., Wang, J., *et al.* (2022) Urban Expansion Weakens the Contribution of Local Land Cover to Urban Warming. *Urban Climate*, **45**, Article ID: 101285. https://doi.org/10.1016/j.uclim.2022.101285

[66] Bailis, R., Ezzati, M. and Kammen, D.M. (2003) Greenhouse Gas Implications of Household Energy Technology in Kenya. *Environmental Science & Technology*, **37**, 2051-2059. https://doi.org/10.1021/es026058q

[67] Grimmond, S. (2007) Urbanization and Global Environmental Change: Local Effects of Urban Warming. *The Geographical Journal*, **173**, 83-88. https://doi.org/10.1111/j.1475-4959.2007.232_3.x

[68] Marshall, B., Ezekiel, C., Gichuki, J., Mkumbo, O., Sitoki, L. and Wanda, F. (2013) Has Climate Change Disrupted Stratification Patterns in Lake Victoria, East Africa? *African Journal of Aquatic Science*, **38**, 249-253. https://doi.org/10.2989/16085914.2013.810140

[69] Liu, L., Cheng, Y., Wang, S., Wei, C., Pöhlker, M.L., Pöhlker, C., *et al.* (2020) Impact

of Biomass Burning Aerosols on Radiation, Clouds, and Precipitation over the Amazon: Relative Importance of Aerosol-Cloud and Aerosol-Radiation Interactions. *Atmospheric Chemistry and Physics*, **20**, 13283-13301. https://doi.org/10.5194/acp-20-13283-2020

[70] Endris, H.S., Lennard, C., Hewitson, B., Dosio, A., Nikulin, G. and Artan, G.A. (2018) Future Changes in Rainfall Associated with ENSO, IOD and Changes in the Mean State over Eastern Africa. *Climate Dynamics*, **52**, 2029-2053. https://doi.org/10.1007/s00382-018-4239-7

[71] Camberlin, P. (2018) Climate of Eastern Africa. Oxford Research Encyclopaedia of Climate Science. https://doi.org/10.1093/acrefore/9780190228620.013.512

[72] Ouma, J.O., Olang, L.O., Ouma, G.O., Oludhe, C., Ogallo, L. and Artan, G. (2018) Magnitudes of Climate Variability and Changes over the Arid and Semi-Arid Lands of Kenya between 1961 and 2013 Period. *American Journal of Climate Change*, **7**, 27-39. https://doi.org/10.4236/ajcc.2018.71004

[73] Ongoma, V., Chen, H. and Omony, G.W. (2016) Variability of Extreme Weather Events over the Equatorial East Africa, a Case Study of Rainfall in Kenya and Uganda. *Theoretical and Applied Climatology*, **131**, 295-308. https://doi.org/10.1007/s00704-016-1973-9

[74] Amou, M., Gyilbag, A., Demelash, T. and Xu, Y. (2020) Heatwaves in Kenya 1987-2016: Facts from CHIRTS High Resolution Satellite Remotely Sensed and Station Blended Temperature Dataset. *Atmosphere*, **12**, Article No. 37. https://doi.org/10.3390/atmos12010037

[75] Longo, L., Birarda, G., Cagnato, C., Badetti, E., Covalenco, S., Pantyukhina, I., *et al.* (2022) Coupling the Beams: How Controlled Extraction Methods and Ftir-Spectroscopy, OM and SEM Reveal the Grinding of Starchy Plants in the Pontic Steppe 36,000 Years Ago. *Journal of Archaeological Science: Reports*, **41**, Article ID: 103333. https://doi.org/10.1016/j.jasrep.2021.103333